Published in final edited form as:
J Am Chem Soc. 2007 August 01; 129(30): 9468–75. doi:10.1021/ja072346g.

Modulation of Heme Redox Potential in the Cytochrome c_6 Family

Jonathan A. R. Worrall[*,†], **Beatrix G. Schlarb-Ridley**[†], **Torsten Reda**[‡], **Maria J. Marcaida**[†], **Robert J. Moorlen**[†], **Juergen Wastl**[†], **Judy Hirst**[‡], **Derek S. Bendall**[†], **Ben F. Luisi**[†], **Christopher J. Howe**[†]

Contribution from the Department of Biochemistry, University of Cambridge, Cambridge, CB2 1GA, U.K., and Medical Research Council Dunn Human Nutrition Unit, Hills Road, Cambridge, CB2 2XY, U.K.

[†]University of Cambridge

[‡]Medical Research Council, Dunn Human Nutrition Unit

Abstract

Cytochrome c_{6A} is a unique dithio-cytochrome of green algae and plants. It has a very similar core structure to that of bacterial and algal cytochromes c_6 but is unable to fulfill the same function of transferring electrons from cytochrome *fto* photosystem I. A key feature is that its heme midpoint potential is more than 200 mV below that of cytochrome c_6 despite having His and Met as axial heme-iron ligands. To identify the molecular origins of the difference in potential, the structure of cytochrome c_6 from the cyanobacterium *Phormidium laminosum* has been determined by X-ray crystallography and compared with the known structure of cytochrome c_{6A}. One salient difference of the heme pockets is that a highly conserved Gln (Q51) in cytochrome c_6 is replaced by Val (V52) in c_{6A}. Using protein film voltammetry, we found that swapping these residues raised the c_{6A} potential by +109 mV and decreased that of c_6 by almost the same extent, -100 mV. X-ray crystallography of the V52Q protein showed that the Gln residue adopts the same configuration relative to the heme as in cytochrome c_6 and we propose that this stereochemistry destabilizes the oxidized form of the heme. Consequently, replacement of Gln by Val was probably a key step in the evolution of cytochrome c_{6A} from cytochrome *c*6, inhibiting reduction by the cytochrome b_6f complex and facilitating establishment of a new function.

Introduction

Cytochromes *c* are involved in many different biological electron transfer (ET) reactions. The most important functional characteristic of any individual cytochrome (cyt) is its midpoint redox potential (E_m). Unfolded mitochondrial cyt *c* has $E_{m,7} \approx -150$ mV, but in the folded protein this increases dramatically to +260 mV.[1] Thus, exclusion of solvent and the structure of the protein environment are of crucial importance in determining the E_m of the native protein. In different *c*-type cyts $E_{m,7}$ ranges between ~ – 400 mV and +400 mV, but in any homologous group of cyts of similar function the redox potential is tuned to a

jw510@mole.bio.cam.ac.uk.

Europe PMC Funders Author Manuscripts

relatively narrow range of values. Such conservation of E_m must depend upon conservation of stereochemistry of the heme pocket, and hence of the amino acid sequence, but a completely satisfactory description has not yet been achieved.

In all Class I cyts *c* the heme is bound near the protein N-terminus by the motif –CXXCH–, in which the His is one of the axial heme ligands. The redox potential is determined by the relative stabilities of the iron-porphyrin ring system in the reduced form, which is electrically neutral, and the oxidized form that carries a positive charge. The nature of the sixth ligand divides Class I cyts into a low-potential group, in which coordination is with the imidazole side chain of a His residue, and a high-potential group that uses the S^{δ} atom of a Met. In mitochondrial cyt *c* an extensive hydrogen bond network, which includes a conserved water molecule (wat166) and several conserved amino acids, is important in determining the redox potential.[2,3]

Cyt *c*6 has a relatively simple hydrogen bond network surrounding the heme cavity, and there is no redox dependent conformational change[4] as observed with mitochondrial cyt *c*.[3] This family of cyts *c* falls into two sections, “conventional” cyt c_6 and cyt c_{6A}, with $E_{m,7}$ values of ~+340 mV for c_6 and ~+100 mV for c_{6A},[5] putting them at opposite ends of the redox potential scale of cyts *c* with His and Met as the axial ligands. Cyt c_6 functions interchangeably with the copper-protein plastocyanin as the electron donor to photosystem I in cyanobacteria and algae, with the relative levels of the two proteins determined by copper availability.[6–8] In green plants, plastocyanin is an essential component of the photosynthetic electron transport chain, so the discovery in *Arabidopsis thaliana* of a gene encoding a cyt c_6-like protein was a surprise.[9,10] Amino acid sequence and structure place the corresponding protein in the c_6 family, and the three-dimensional structure of the *A. thaliana* protein confirms a high structural similarity with cyt c_6 from algal and cyanobacterial sources as well as the presence of His and Met as axial ligands to the heme iron.[5,11] The most striking structural difference from algal and cyanobacterial cyt c_6, which was also inferred from sequence analysis, is the presence of a surface exposed 12 residue loop insertion peptide (LIP) containing a disulfide bridge between Cys67 and Cys73. In view of these differences, the novel form of the protein has been named cyt c_{6A}.

In spite of the similarity between cyt c_{6A} and conventional cyt c_6, the former is unable to replace the function of plastocyanin. Unlike plastocyanin and cyt c_6, it is only slowly oxidized by photosystem I,[12] and its low redox potential makes it unable to oxidize the cyt b_6f complex. The natural reductant of cyt c_{6A} remains unidentified. However, if the redox potential of the heme in cyt c_{6A} remained similar to that of the ancestral cyt c_6, reduction by the cyt b_6f complex would still be possible, even though the role of the newly evolved cyt c_{6A} was to be reduced by something else. Continued reduction by the cyt b_6f complex would presumably compromise the new function of cyt c_{6A}. The evolution of an unusually low redox potential for the heme in cyt c_{6A} can therefore be seen as an important step in the development of a novel function for the protein. The aim of the present work was to identify the origin(s) of the difference in E_m between cyt c_{6A} and cyt c_6.

We have determined the X-ray structure of a cyt c_6 from the cyanobacterium *Phormidium laminosum* and compared the heme pocket to that of *A. thaliana* cyt c_{6A}. This reveals a

number of subtle differences which have been probed by site-directed mutagenesis, protein film voltammetry, and X-ray crystallography. This study has revealed that a single residue, which is not a heme ligand, is responsible for tuning the heme redox potential by ~100 mV. We suggest that mutation of this residue was a crucial step in the evolution of cyt c_{6A} from cyt c_6.

Materials and Methods

Expression Plasmid for *P. laminosum* cyt c_6

Recombinant *P. laminosum* cyt c_6 was obtained by expression in *Escherichia coli* of a synthetic gene containing the coding region of the mature *P. laminosum* cyt c_6 fused to the signal peptide from *Anabaena* cyt c_6 (the sequence of this synthetic gene is reported in the Supporting Information). The synthetic gene was generated by back-translation of the amino acid sequence and the codon usage of *E. coli* genes that are highly expressed during exponential growth. The product was cloned into pGEMT-easy for expression under the T7-promoter. Correct sequence and direction of insertion were confirmed by sequencing. The resulting expression plasmid was named pPlc6.

Site-Directed Mutagenesis

Mutations were introduced using the Stratagene QuikChange method.[13] The mutants V52Q and V52Q-AA of the *A. thaliana* cytochrome c_{6A} gene were generated by replacing the codon “GTG” in the wild-type or I17A/G18A cyt c_{6A} expression plasmids (pAtc6a and pAtc6aAA, respectively)[5] by “CAG”. Mutant A31K was generated by replacing the codon “GCG” in plasmid pAtc6a by “AAA”. The mutant Q51V of the *P. laminosum* cyt c_6 gene was generated by replacing the codon “CAG” in the expression plasmid pPlc6 by “GTG”. Incorporation of the correct mutations and absence of undesired changes were corroborated by sequencing of the mutated constructs.

Protein Expression and Purification

Wild-type and mutant *A. thaliana* cyt c_{6A} were expressed and purified as described in ref 5. Expression of wild-type and mutant *P. laminosum* cyt c_6 differed as follows: *E. coli* BL21(DE3) was used instead of GM119, and expression cultures were induced with 100 mg/L IPTG after overnight growth at 30 °C and 170 rpm. Purification was analogous to the procedure used for *A. thaliana* cyt c_{6A}.

Crystallization and X-ray Data Collection

Crystals of *P. lami- nosum* cyt c_6 and *A. thaliana* cyt c_{6A} V52Q-AA variant were grown by the hanging drop vapor diffusion method with 1 μL of protein solution mixed with 1 μL of reservoir solution. For *P. laminosum* cyt c_6 the reservoir solution contained 2.5 M NaCl, 100 mM imidazole, 200 mM $Zn(OAc)_2$, pH 6.0. For *A. thaliana* cyt c_{6A} V52Q-AA variant, 1.26 M ammonium sulfate, 100 mM acetate pH 4.5, and 200 mM NaCl were used as precipitant. Prior to data collection, protein crystals were immersed in their respective precipitant solution containing 20% v/v glycerol, followed by rapid freezing in liquid nitrogen. X-ray diffraction data were collected on beamline ID 29-1 at the ESRF Grenoble, France. Data were indexed, integrated, and scaled with Denzo and Scalepack.[14]

Structure Determination and Refinement

Molecular replacement was used to solve both structures. The program PHASER was employed[15] for *P. laminosum* cyt c_6, using the structure of *M. braunii* cyt c_6 (PDB entry 1ctj) as a search model.[16] Data collected at the Feedge were useful to corroborate the position of the Fe atom in the maps and for modeling using anomalous Fourier synthesis. For the V52Q-AA variant the program MOLREP[17] was used in conjunction with the oxidized wild-type-AA cyt c_{6A} structure (PDB code 2ce0) as the search model.[5] A solution was obtained with an *R*-factor of 36.2% and a correlation coefficient of 65.0%. For both structures several rounds of rigid body and restrained refinement were carried out with REFMAC5[18] followed by automatic building of waters in ARP/WARP.[19] Iterative cycles of model building with Coot[20] followed by restrained refinement resulted in final models with the statistics reported in Table 1. The coordinates and structure factors have been deposited in the Protein Data Bank under the accession codes 2v08 (r2v08sf) for *P. laminosum* cyt c_6 and 2v07 (r2v07sf) for *A. thaliana* V52Q-AA cyt c_{6A}. Structure figures were prepared using the program Pymol.[21]

Protein Film Voltammetry

Reduction potentials were measured by protein film voltammetry as described previously.[22] All potentials are reported relative to the standard hydrogen electrode.

Results

Crystal Structure of Reduced *P. laminosum* cyt c_6 and Comparison of the Heme Pocket with *A. thaliana* cyt c_{6A}

Reduced crystals of *P. laminosum* cyt c_6 contain two protein molecules in the asymmetric unit (chains A and B: residues 3–86) with the Cα-atoms of the two chains superimposing with a root-mean-square deviation (rmsd) of 0.09 Å. Statistics for data collection and refinement are summarized in Table 1. The two molecules form a dimer with an interface which is small (294 $Å^2$), poorly packed, and largely hydrophobic (78% apolar atoms). An Fe–Fe distance of 16.2 Å and nonplanar orientation of the two hemes suggest optimization for fast intermolecular ET. A high interface planarity is also calculated indicative of weak interactions within the homodimer interface.[23,24] The overall fold of each monomer is homologous to other cyts c_6 (Figure 1), and the backbone can be superimposed on that of cyt c_{6A} (excluding the LIP) with an rmsd of 1.3 Å. The heme iron is coordinated via the $N^{\epsilon 1}$ of H19 and the S^{δ} of M59, with the latter having a *trans* orientation along the C^{β}–C^{γ} bond, with R stereochemistry at the pro-chiral sulfur ligand. No hydrogen bond interaction to the S^{δ} atom of the Met ligand is observed.

In both *P. laminosum* cyt c_6 and *A. thaliana* cyt c_{6A} the heme environment is predominantly hydrophobic, although differences in residue properties occur at postions 31, 41, 52, and 53 (*A. thaliana* numbering, Figure 2A) which may influence the heme E_m value. A water molecule, interconnecting the heme propionates via hydrogen bonds, is observed in both structures (Figure 2). This water is structurally conserved in all cyt c_6 structures, but there is no evidence to suggest that it moves upon change of oxidation state in cyt c_{6A} or cyt c_6.[4,5] A structural rearrangement involving a water molecule contributes to stabilizing the

positively charged oxidized heme in the mitochondrial cyts *c*.[2,3] The most extensive polar interactions are in the heme pocket of *P. laminosum* cyt c_6 (Figure 2 and Table S1 Supporting Information) which is dominated by the Q51 side chain. This is fixed into position by a hydrogen bond with the conserved water molecule and pinions the side chain so that its $N^{\epsilon 2}$ atom is in van der Waals contact (3.0 Å) with a methine carbon atom of the porphyrin ring (Figure 2B).

The absence of the Gln residue is the predominant feature distinguishing the heme pocket of cyt c_{6A} from cyts c_6 (Figure 2B,C). No electrostatic interaction involving an electropositive amino acid side chain and a heme propionate is present in cyt c_{6A}, whereas a hydrogen bond between the heme propionate-6 and the side chain N^{ζ} of K30 is present in *P. laminosum* cyt c_6 (Figure 2B, Table S1 Supporting Information). An electropositive side chain in this position is highly conserved within the cyt c_6 family but is an Ala (A31 in *A. thaliana)* or Ser in all known cyt c_{6A} sequences. The presence of a strongly electron withdrawing group interacting with a heme propionate would be expected to affect the heme E_m [25,26] by electrostatic destabilization of the positive charge on the oxidized cyt and by a downward shift of the propionate pK in the oxidized form. Based on these differences, single-site variants were constructed in *P. laminosum* cyt c_6 (Q51V-c_6) and *A. thaliana* cyt c_{6A} (V52Q-c_{6A} and A31K-c_{6A}) to explore the individual contributions of these molecular substitutions on heme E_m in the c_6 family.

Variations in the Heme Reduction Potentials

Typical cyclic voltammograms recorded for *P. laminosum* cyt c_6 and *A. thaliana* cyt c_{6A} are shown in Figure 3A. The small peak-to-peak separations observed (30–50 mV) confirm that the proteins were adsorbed onto the pyrolytic graphite edge (PGE) electrode surface, and the E_m values are taken from the average of the reductive and oxidative peak potentials. Table 2 reports the pH-independent E_m values for each protein, observed at close to neutral pH. The potential for *A. thaliana* cyt c_{6A} is ~250 mV lower than that of *P. laminosum* cyt c_6 which in thermodynamic terms corresponds to ~6 kcal/mol in the free energy of oxidation of the ferrous heme ($\Delta G°$). For V52Q-c_{6A} an increase in *E*m of 109 mV is observed (Table 2), and an almost corresponding decrease is observed in the converse mutation (Q51V) in *P. laminosum* cyt c_6 (Table 2). Thus the Gln to Val mutation has accounted for almost half the difference in redox potential between cyt c_6 and cyt c_{6A}. Interestingly, residue 51/ 52 (Gln/ Val), which lies close to the porphyrin ring, is responsible for the 2 nm bathochromic shift of the α-band in cyt c_{6A} (Table 2). Insertion of an electropositive residue in the vicinity of the heme propionate-6 in cyt c_{6A} (A31K) raises the E_m of the heme (Table 2). However, this increase is only a third of that observed for the Val to Gln mutation in cyt c_{6A} (Table 2).

In each case variation of E_m with pH displays three phases (Figure 3B). The physiologically significant pH range is probably 5 to 7, mostly in the pH independent region. The “low-pH” transition has been characterized using the Nernst equation for a single protonation event[27] using two pK values, pK_{ox1} and pK_{red1}, referring to the oxidized and reduced states, respectively (Table 2). pK_{ox1} and pK_{red1} probably refer to one of the heme propionates, most likely the less-solvent-exposed propionate-7, in analogy to other *c*-type cyts.[28,29] The pK_1 values for V52Q-c_{6A} and Q51V-c_6 are similar to those of their respective wild-type

proteins, but the separation between p*K*ox1 and p*K*red1 is considerably larger for cyt c_{6A} (1.5) than c_6 (0.7), indicating increased interaction between the sites of electronation and protonation. The introduction of the positive charge with the A31K-c_{6A} mutant might be expected to lower pK_{ox1}, whereas a small increase was actually observed (Table 2).

The "alkaline transition" described by pK_{ox2} occurs at a variable pH (Table 2) and has been modeled similarly by a coupled deprotonation event. The variants of each species show significant variations in their pK_{ox2} values, though the Q51V mutation shifts the value of *P. laminosum* cyt c_6 toward that of *A. thaliana* cyt c_{6A}, and the A31K-c_{6A} mutation shifts the value of *A. thaliana* cyt c_{6A} toward that of *P. laminosum* cyt c_6.

Redox Potential and Structure of the Oxidized V52Q-AA Variant of *A. thaliana* cyt c_{6A}

The double Ala variant, I17A-G18A (AA), was used to study the structure of the V52Q-c_{6A} mutation. The reason for using the double AA mutation is that it crystallizes with a simpler unit cell and higher crystallographic order than the wild-type protein.[5,11] The double AA mutations lie in the – CXXCH– heme binding motif and have minimal effect on the structure of cyt c_{6A} compared to the wild-type protein.[5,11] Two Ala residues are found in the corresponding positions in *P. laminosum* cyt c_6 (Figure 2A) and many other cyts c_6. The effect on E_m for the AA substitutions in cyt c_{6A} compared to the wild-type protein is small, with a slight increase in E_m being observed (Table 2). The V52Q-AA-c_{6A} variant shows a large increase in E_m over the AA variant, as observed between the wild-type protein and the V52Q-c_{6A} variant. The effect is a little smaller in the AA background than in the wild type (97 mV compared with 109 mV). The AA-c_{6A} and V52Q-AA-c_{6A} variants also display small shifts in the pK values (Table 2).

The structure of the oxidized V52Q-AA-c_{6A} variant was refined at 1.6 Å resolution; statistics for data collection and refinement are summarized in Table 1 and electron density shown in Figure 4A. Unambiguous electron density for a Gln residue was observed in difference maps of the V52Q-AA-c_{6A}, when using the AA-c_{6A} structure as the search model.[5] Figure 4B compares the structures of the heme cavities in V52Q-AA-c_{6A} and *P. laminosum* cyt c_6. The side-chain orientation of Q52 is similar to the "naturally' occurring Gln residue in *P. laminosum* cyt c_6 with the $N^{\epsilon 2}$ atom hydrogen bonding with the structurally conserved bridging propionate water. This bridging water, a conserved presence throughout the c_6 structural family, facilitates orientation of the Gln side-chain amide group to within van der Waals contact (3.2 Å) of a methine carbon of the porphyrin ring. Additional small structural differences between V52Q-AA-c_{6A} and the AA-c_{6A} are confined to the periphery of the heme pocket. In V52Q-AA-c_{6A} the heme propionate-6 carboxyl groups are perpendicular instead of parallel to the heme plane producing small changes in length of hydrogen bonds from the atom O2D (Figure 4B and Table S1). This structural change also results in another water molecule bridging the two heme propionates (Figure 4B and Table S1). At the distal side of the heme, the axial heme ligand, M60, rearranges from a *trans* to a *cis* conformation along the C^{β}-C^{γ} bond retaining the same stereochemistry at the chiral sulfur (Figure 4A), but shifting slightly the main-chain atoms of M60 and P61.

Calculations of the Solvent Exposure of the Hemes in cyts c_6 and c_{6A}

Differences in the solvent exposure of the heme in cyts c_6 and c_{6A} may contribute to the large difference in reduction potential (see Table 3). The total exposure of the heme is dominated by that of propionate-6. However, the propionic acid side chain is not part of the conjugated ring system, and its main effect on E_m is the result of electrostatic stabilization of the ferric heme state;[28,30] in all cases studied the propionate remains mainly charged in the pH range 6–7. Alternatively, calculating the solvent exposure for the iron-porphyrin ring system and atoms within one α-bond of the ring, as suggested by Tezcan et al.,[1] may prove more meaningful (see Table 3). The smaller areas of exposure result largely from the methyl-3 carbon atom. Although the cyts c_6 mostly show lower exposures than cyt c_{6A}, by both criteria the spread of values is wide and the number of samples for cyt c_{6A} small. The V52Q-AA-c_{6A} substitution increased the total heme exposure but had an insignificant effect on the porphyrin ring exposure, perhaps because of the slight readjustment in the position of the main chain discussed above.

Discussion

As part of the present work we have determined the structure of reduced cyt c_6 from the cyanobacterium *P. laminosum* which reveals a homodimer in the asymmetric unit. The overall fold and heme architecture are very similar to other cyts c_6 for which structures are known. Homodimers in the solid and solution state have been reported for other cyts c_6.[4,31,32] However in the solid state none has interface properties resembling a transient ET complex as is observed here for *P. laminosum* cyt c_6. The *P. laminosum* cyt c_6 monomer was used to search for the molecular origins of the difference in heme redox potential displayed between cyt c_6 and cyt c_{6A}. At physiological pH the latter has an *E*m of +71 mV measured using PFV and is the lowest for a naturally occurring cyt *c* with His and Met as heme axial ligands. This potential is more in line with bis-His cyts where the replacement of the axial Met with a His residue results in a downward shift in potential as observed in the semisynthetic bis-His cyt *c*.[33] Thus the low heme midpoint potential of cyt c_{6A} suggests that factors other than the nature of the axial ligand are responsible.

Residue 51/52 is a major regulator of E_m between cyt c_6 and cyt c_{6A}

Removal of the polar Gln and replacement with the hydrophobic Val, as found “naturally” in many cyts c_{6A}, would *a priori* have been predicted to increase the heme redox potential, as the positive charge on the oxidized heme is destabilized by the increased hydrophobicity. However, the effect is the opposite. In all known cyt c_6 structures and in the V52Q-AA-c_{6A} variant, the conserved Gln side chain is hydrogen bonded to a structurally conserved water molecule. This water locks the side chain into an orientation in which the amide group is pointing toward the porphyrin ring and within van der Waals distance of a methine carbon on the porphyrin ring. We suggest that this positioning of the Gln side chain is responsible for ~100 mV of heme redox potential in the cyts c_6, with the conserved water having an important structural role.

One possibility is that the amide group of the Gln and the porphyrin ring form an unusual aromatic hydrogen bond (one proton from the amide group (the donor) points toward a ring

carbon atom (the acceptor)). Aromatic hydrogen bonds are estimated to have half the strength of conventional hydrogen bonds.[34] Such an interaction could perturb the electron spin density of the porphyrin ring and so influence the redox potential. Amide/aromatic H-bonds have a larger interplanar angle between the ring perpendicular and the donor than the more common amide/aromatic stacking interactions, a separation of less than 3.8 Å between the donor (the sp^2 nitrogen) and acceptor, and an N–H···C angle greater than 120°.[35] In both *P. laminosum* cyt c_6 and the V52Q-AA-c_{6A} structures, the sp^2 hybridized nitrogen of the Gln side chain is less than 3.5 Å from the ring carbon of the aromatic porphyrin, with a N–H···C of ~105°. Thus the interaction does not quite fulfill all the criteria for an amide/aromatic hydrogen bond, but the van der Waals contact does suggest that it is a key determinant of the physical properties of the porphyrin. This is consistent with the spectral shift caused by the presence of the Gln residue (Table 2) which is a clear indication that it interacts with the π-electron system of the porphyrin ring.[36]

A second possibility is a simple dipolar interaction with the polar Gln side chain destabilizing the positively charged oxidized heme. A similar electrostatic interaction has been reported in mitochrondrial cyts *c* involving a side chain dipole of an Asn and a water molecule.[37] Upon substitution of the Asn for an Ile the water molecule in the heme pocket is lost together with the side chain dipole. This results in a smaller destabilization of the oxidized state and a 55 mV decrease in E_m.[37]

Other Contributors to the Differences in E_m between cyt c_6 and cyt c_{6A}

Although the Gln/Val substitution results in a significant change in reduction potential, it does not account for all of the difference (~ 250 mV) between cyt c_6 and cyt c_{6A}. Other factors which may be important are the electron spin-density distribution in the porphyrin ring system, the Fe–$S^{\delta-}$ (Met) bond strength, further electrostatic interactions, and heme solvent exposure. In V52Q-AA-c_{6A} a change in the side chain orientation of M60 from *trans* to *cis* is observed (Figure 4A) with the stereochemistry of the sulfur atom retained. This change in orientation of the Met ligand will influence the electronic structure of the porphyrin which in turn could have an influence on the E_m.[38] However, from extensive work by Walker and co-workers the axial ligand orientation is expected to have only a small effect on the heme E_m in cyts *c*.[39]

Previous structural analysis suggested the electrostatic interaction between an electropositive amino acid side chain and a heme propionate was the key determinant of the decreased reduction potential of cyt c_{6A}.[11] Here, study of the A31K-c_{6A} variant showed that introduction of a positively charged residue does indeed raise the heme's redox potential, but by only 34 mV (Table 2). This substitution could therefore be considered to "fine-tune" the reduction potential, as it does not account for a major part of the difference in potential between cyts c_6 and c_{6A}. Likewise mutation of the corresponding residue in a cyt c_6, K29 to a His resulted in a downward shift in redox potential of 65 mV.[40] Together residues 31 and 51/52 contribute ~ 150 mV of heme redox potential ($\Delta G° \approx 3.5$ kcal/mol) which equates to ~50% of the known accessible redox space sampled in Class I cyts *c* and 60% of the difference between the proteins studied here. Other residues, identified above, which could contribute to a further lowering of redox potential are N41 and T53. The side chain of N41 is

within hydrogen-bonding distance of heme propionate-7, but cyt c_6 from several species also has an Asn in this position. T53 would be expected to have some effect on heme potential, but this would probably be smaller than that of a Gln at position 51/52 because the side chain O^{γ} is not in van der Waals contact with the porphyrin ring and the side chain dipole is smaller than that of Gln. Moreover, cyt c_{6A} of *Chlamydomonas* has Ile instead of Thr in this position.[41]

Differences in the solvent exposure of the porphyrin rings may, in comparison to the results of Tezcan et al.,[1] contribute up to 100 mV to the reduction potential. Although examination of space filling models of the known crystal structures suggests a larger gap adjacent to the heme methyl-3 carbon atom in cyt c_{6A} compared with c_6, we have been unable to find a single residue that is conserved in one group and not in the other and could be responsible for the change in solvent exposure of the heme.

Evolution of Heme Redox Potential in cyt c_{6A} and Its Biological Implications

The original function of cyt c_6 in chloroplasts was to transfer electrons from the cyt b_6f complex to photosystem I (and in photosynthetic bacteria it may also have served as an electron donor to cyt *c* oxidase). Oxidation of the cyt b_6f complex requires a high redox potential. Attempts to modify the redox potential of cyts by site-directed mutagenesis have usually led to a lowering of potential. Lett and Guillemette found only one mutant of yeast iso-1-cyt *c* in which the potential was raised,[25] and McClendon and co-workers found that the potential of wild-type cyt *b*562 lay at the upper end of a range of potentials of mutant forms.[42,43] The same authors suggested that many cyts (and possibly many other redox proteins) have evolved to maximize the redox potential by stabilizing their reduced state relative to the oxidized state, consistent with cyt c_6 accepting electrons from the cyt b_6f complex. By contrast, the evolution of cyt c_{6A} has followed a path of increasing stabilization of the oxidized state relative to the reduced, leading to an unusually low E_m for a cyt *c* with His-Met ligation.

The function of cyt c_{6A} remains unknown, but it is not involved in photosynthetic electron transfer beween the cyt b_6f complex and photosystem I.[12,44] Given the high degree of conservation of residues forming the heme pocket of cyt c_{6A}, it is likely that the low redox potential is a universal feature of the cyt in higher plants. Assuming that oxidation and reduction of the heme are an essential feature of the function of cyt c_{6A}, the lowering of midpoint potential of cyt c_6 by ~100 mV by the Gln to Val substitution is an example of how a single amino acid change could, in principle, alter the properties of the protein to abolish its original function and perform a new one more effectively. Presumably substitution of the Gln would have been preceded by a duplication of the cyt c_6 gene, to allow retention of a "conventional" cyt c_6 for photosynthetic electron transfer, as in *Chlamydomonas.*[41] One form of the protein acquired a new function, perhaps associated with insertion of the cysteine-containing stretch into the LIP. Substitution of the Gln ensured that reduction by the cyt *b6f* complex could not interfere with the new function, and this was probably followed by additional tuning of cyt c_{6A} to lower its midpoint potential further, resulting in the protein seen today.

Supplementary Material

Refer to Web version on PubMed Central for supplementary material.

Acknowledgements

This work was supported by the Wellcome Trust, BBSRC, the Medical Research Council, the Nuffield Foundation, and the Newton Trust. We thank the staff of the European Synchrotron Radiation Facility (ESRF) for support with data collection.

The abbreviations used are as follows

cyt *c*	cytochrome *c*
PGE	pyrolytic graphite edge
LIP	loop insertion peptide
IPTG	Isopropyl-D-thiogalactoside
E_m	midpoint potential
ET	electron transfer

References

(1). Tezcan FA, Winkler JR, Gray HB. J Am Chem Soc. 1998; 120:13383–13388.

(2). Berghuis AM, Brayer GD. J Mol Biol. 1992; 223:959–976. [PubMed: 1311391]

(3). Berghuis AM, Guillemette JG, McLendon G, Sherman F, Smith M, Brayer GD. J Mol Biol. 1994; 236:786–799. [PubMed: 8114094]

(4). Schnackenberg J, Than ME, Mann K, Wiegand G, Huber R, Reuter W. J Mol Biol. 1999; 290:1019–1030. [PubMed: 10438600]

(5). Marcaida MJ, Schlarb-Ridley BG, Worrall JAR, Wastl J, Evans TJ, Bendall DS, Luisi BF, Howe CJ. J Mol Biol. 2006; 360:968–977. [PubMed: 16815443]

(6). Ho KK, Krogmann DW. Biochim Biophys Acta. 1984; 766:310–316.

(7). Merchant S, Bogorad L. Mol Cell Biol. 1986; 6:462–469. [PubMed: 3023849]

(8). Wood PM. Eur J Biochem. 1978; 87:9–19. [PubMed: 208838]

(9). Gupta R, He Z, Luan S. Nature. 2002; 417:567–571. [PubMed: 12037572]

(10). Wastl J, Bendall DS, Howe CJ. Trends Plant Sci. 2002; 7:244–245. [PubMed: 12049919]

(11). Chida H, Yokoyama T, Kawai F, Nakazawa A, Akazaki H, Takayama Y, Hirano T, Suruga K, Satoh T, Yamada S, Kawachi R, et al. FEBS Lett. 2006; 580:3763–3768. [PubMed: 16777100]

(12). Molina-Heredia FP, Wastl J, Navarro JA, Bendall DS, Hervas M, Howe CJ, De La Rosa MA. Nature. 2003; 424:33–34.

(13). Braman J, Papworth C, Greener A. Methods Mol Biol. 1996; 57:3144.

(14). Otwinowski Z, Minor W. Methods Enzymol. 1997; 276:307–326.

(15). McCoy AJ, Grosse-Kunstleve RW, Storoni LC, Read RJ. Acta Crystallogr, Sect D. 2005; 61:458–464. [PubMed: 15805601]

(16). Frazao C, Soares CM, Carrondo MA, Pohl E, Dauter Z, Wilson KS, Hervas M, Navarro JA, De la Rosa MA, Sheldrick GM. Structure. 1995; 3:1159–1169. [PubMed: 8591027]

(17). Vagin A, Teplyakov A. J Appl Crystallogr. 1997; 30:1022–1025.

(18). Murshudov GN, Vagin AA, Dodson EJ. Acta Crystallogr, Sect D. 1997; 53:240–255. [PubMed: 15299926]

(19). Perrakis A, Sixma TK, Wilson KS, Lamzin VS. Acta Crystallogr, Sect D. 1997; 53:448–455. [PubMed: 15299911]
(20). Emsley P, Cowtan K. Acta Crystallogr, Sect D. 2004; 60:2126–32. [PubMed: 15572765]
(21). DeLano, WL. The Pymol Molecular Graphics Systems. San Carlos, CA, U.S.A: 2002.
(22). Leggate EJ, Hirst J. Biochemistry. 2005; 44:7048–7058. [PubMed: 15865449]
(23). Nooren IM, Thornton JM. J Mol Biol. 2003; 325:991–1018. [PubMed: 12527304]
(24). Sato K, Crowley PB, Dennison C. J Biol Chem. 2005; 280:19281–19288. [PubMed: 15743773]
(25). Lett CM, Guillemette JG. Biochem J. 2002; 362:281–287. [PubMed: 11853535]
(26). Lo TP, Komar-Panicucci S, Sherman F, McLendon G, Brayer GD. Biochemistry. 1995; 34:5259–5268. [PubMed: 7711047]
(27). Clark, WM. Oxidation-Reduction Potentials of Organic Systems. Bailliere, Trindall and Cox; London: 1960.
(28). Takayama SJ, Mikami S, Terui N, Mita H, Hasegawa J, Sambongi Y, Yamamoto Y. Biochemistry. 2005; 44:5488–5494. [PubMed: 15807542]
(29). Ye T, Kaur R, Wen X, Bren KL, Elliott SJ. Inorg Chem. 2005; 44:8999–9006. [PubMed: 16296855]
(30). Mao J, Hauser K, Gunner MR. Biochemistry. 2003; 42:9829–9840. [PubMed: 12924932]
(31). Kerfeld CA, Anwar HP, Interrante R, Merchant S, Yeates TO. J Mol Biol. 1995; 250:627–647. [PubMed: 7623381]
(32). Sawaya MR, Krogmann DW, Serag A, Ho KK, Yeates TO, Kerfeld CA. Biochemistry. 2001; 40:9215–9225. [PubMed: 11478889]
(33). Raphael AL, Gray HB. Proteins. 1989; 6:338–340. [PubMed: 2560194]
(34). Levitt M, Perutz MF. J Mol Biol. 1988; 201:751–754. [PubMed: 3172202]
(35). Mitchell JB, Nandi CL, McDonald IK, Thornton JM, Price SL. J Mol Biol. 1994; 239:315–331. [PubMed: 8196060]
(36). Ponamarev MV, Schlarb BG, Howe CJ, Carrell CJ, Smith JL, Bendall DS, Cramer WA. Biochemistry. 2000; 39:5971–5976. [PubMed: 10821668]
(37). Langen R, Brayer GD, Berghuis AM, McLendon G, Sherman F, Warshel A. J Mol Biol. 1992; 224:589–600. [PubMed: 1314900]
(38). Shokhirev NV, Walker FA. J Biol Inorg Chem. 1998; 3:581–594.
(39). Walker FA, Huyuh BH, Scheidt WR, Osvath SR. J Am Chem Soc. 1986; 108:5298–5297.
(40). De la Cerda B, Diaz-Quintana A, Navarro JA, Hervas M, De la Rosa MA. J Biol Chem. 1999; 274:13292–13297. [PubMed: 10224089]
(41). Wastl J, Purton S, Bendall DS, Howe CJ. Trends Plant Sci. 2004; 9:474–476. [PubMed: 15465681]
(42). Springs SL, Bass SE, Bowman G, Nodelman I, Schutt CE, McLendon GL. Biochemistry. 2002; 41:4321–4328. [PubMed: 11914078]
(43). Springs SL, Bass SE, McLendon GL. Biochemistry. 2000; 39:6075–6082. [PubMed: 10821680]
(44). Weigel M, Varotto C, Pesaresi P, Finazzi G, Rappaport F, Salamini F, Leister D. J Biol Chem. 2003; 278:31286–31289. [PubMed: 12773541]
(45). Kyte J, Doolittle RF. J Mol Biol. 1982; 157:105–132. [PubMed: 7108955]
(46). Clamp M, Cuff J, Searle SM, Barton GJ. Bioinformatics. 2004; 20:426–427. [PubMed: 14960472]
(47). Cho YS, Wang QJ, Krogmann D, Whitmarsh J. Biochim Biophys Acta. 1999; 1413:92–97. [PubMed: 10514550]
(48). Dikiy A, Carpentier W, Vandenberghe I, Borsari M, Safarov N, Dikaya E, Van Beeumen J, Ciurli S. Biochemistry. 2002; 41:14689–14699. [PubMed: 12475218]
(49). Gorman DS, Levine RP. Plant Physiol. 1966; 41:1637–1642. [PubMed: 16656451]
(50). Campos AP, Aguiar AP, Hervas M, Regalla M, Navarro JA, Ortega JM, Xavier AV, De La Rosa MA, Teixeira M. Eur J Biochem. 1993; 216:329–41. [PubMed: 8396033]
(51). Yamada S, Park SY, Shimizu H, Koshizuka Y, Kadokura K, Satoh T, Suruga K, Ogawa M, Isogai Y, Nishio T, Shiro Y, et al. Acta Crystallogr, Sect D. 2000; 56:1577–1582. [PubMed: 11092924]

(52). Hubbard, SJ, Thornton, JM. NACCESS, Computer program. Department of Biochemistry and Molecular Biology, University College; London: 1993.

Europe PMC Funders Author Manuscripts

Europe PMC Funders Author Manuscripts

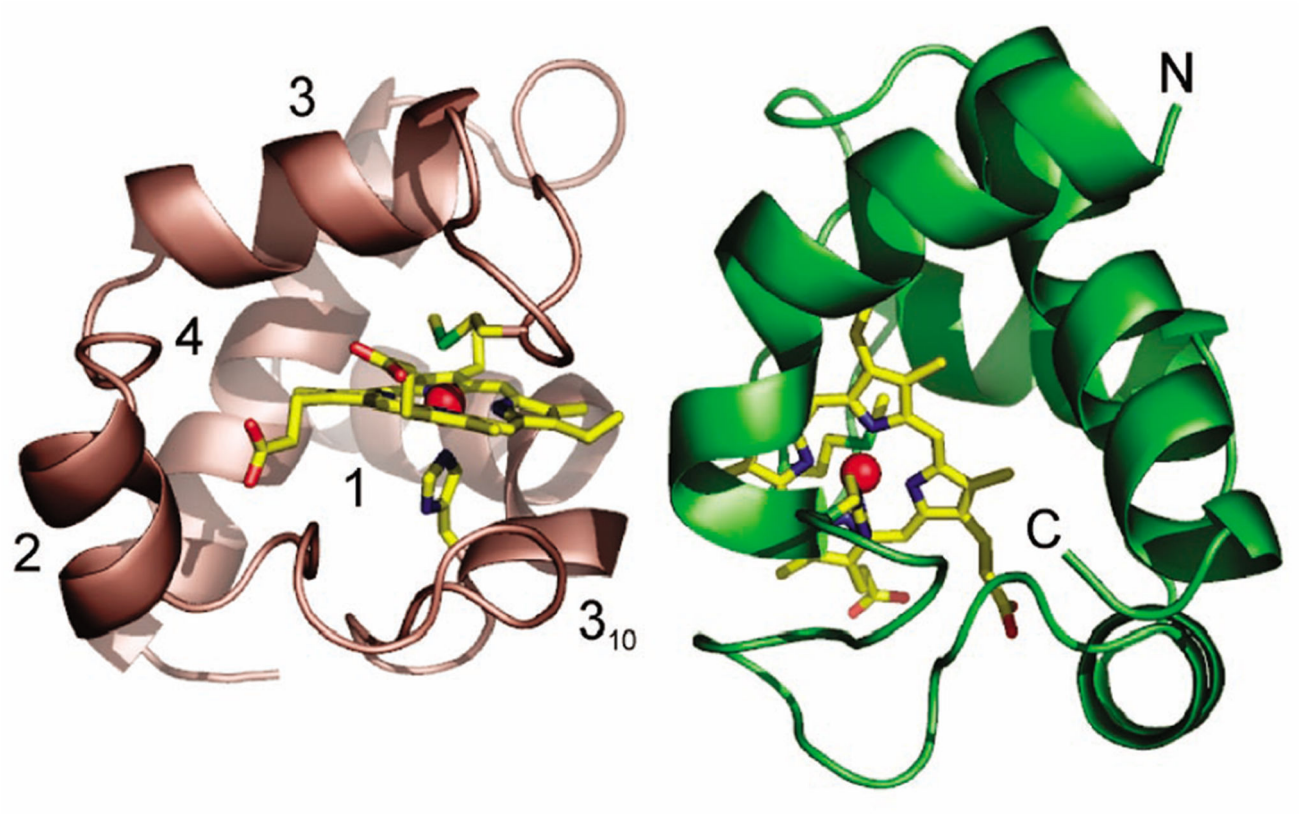

Figure 1. Three-dimensional structure of the homodimer of reduced *P. laminosum* cyt c_6.
Chains A and B are colored green and salmon, respectively. The heme and axial ligands are in stick representation with the Fe as a red sphere. Each monomer is composed of four α-helices, three β-turns, and one γ-inverse turn. Helix 1 is distorted at C15 with residues 15–18 part of a 310 helix fragment. The N and C terminal helices are indicated for chain A.

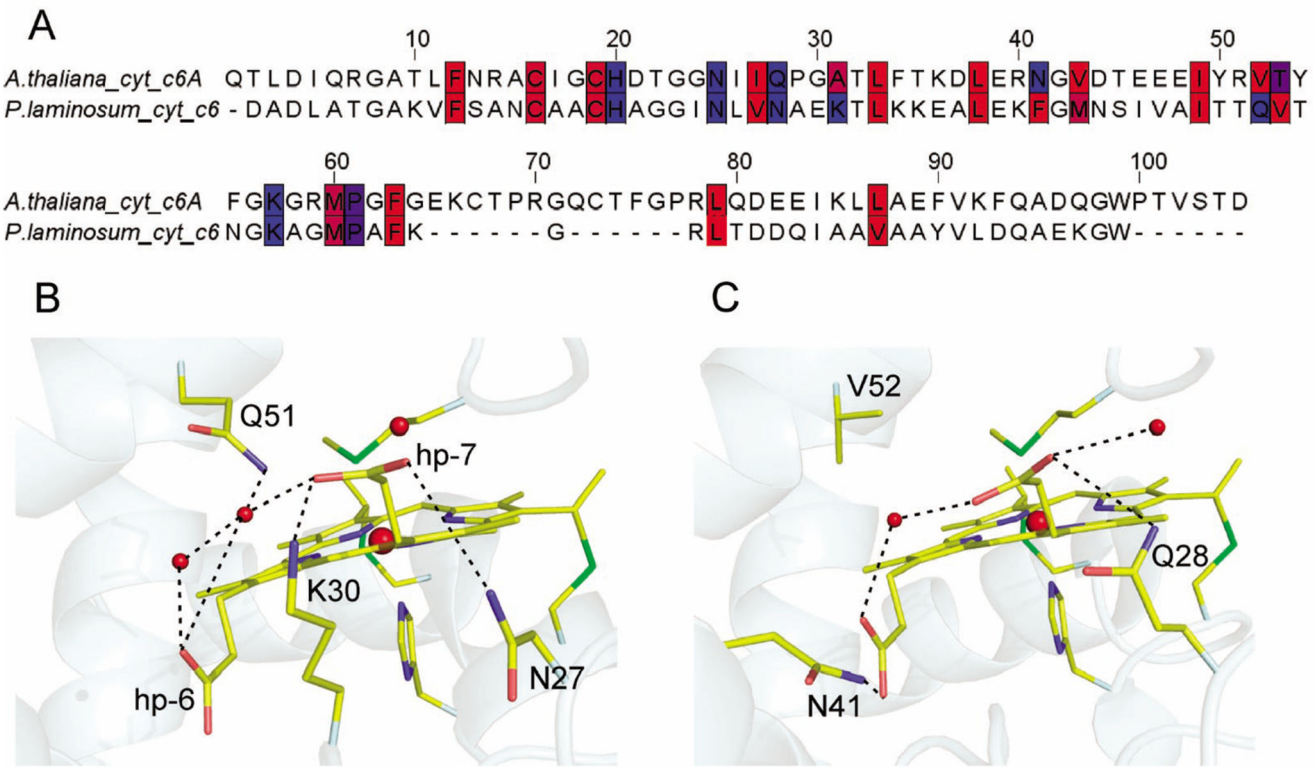

Figure 2. Structural comparison of the heme binding sites.

(A) Sequence alignment between *A. thaliana* cyt c_{6A} and *P. laminosum* cyt c_6 (sequence identity 34%). Residues whose side-chain atoms are within 5 Å of a heme atom are colored red to blue according to their hydrophobicity (blue = most polar, red = least polar),[45] using the JalView alignment editor.[46] (B and C) The heme binding pockets of reduced *P. laminosum* cyt c_6 and reduced *A. thaliana* cyt c_{6A}, respectively. Water molecules are shown as small red spheres with the predominant polar interactions indicated by dashed lines; the larger spheres are the heme iron. The heme propionates are assigned as hp. A summary of the respective heme cavity polar interactions is given in Table S1.

Europe PMC Funders Author Manuscripts

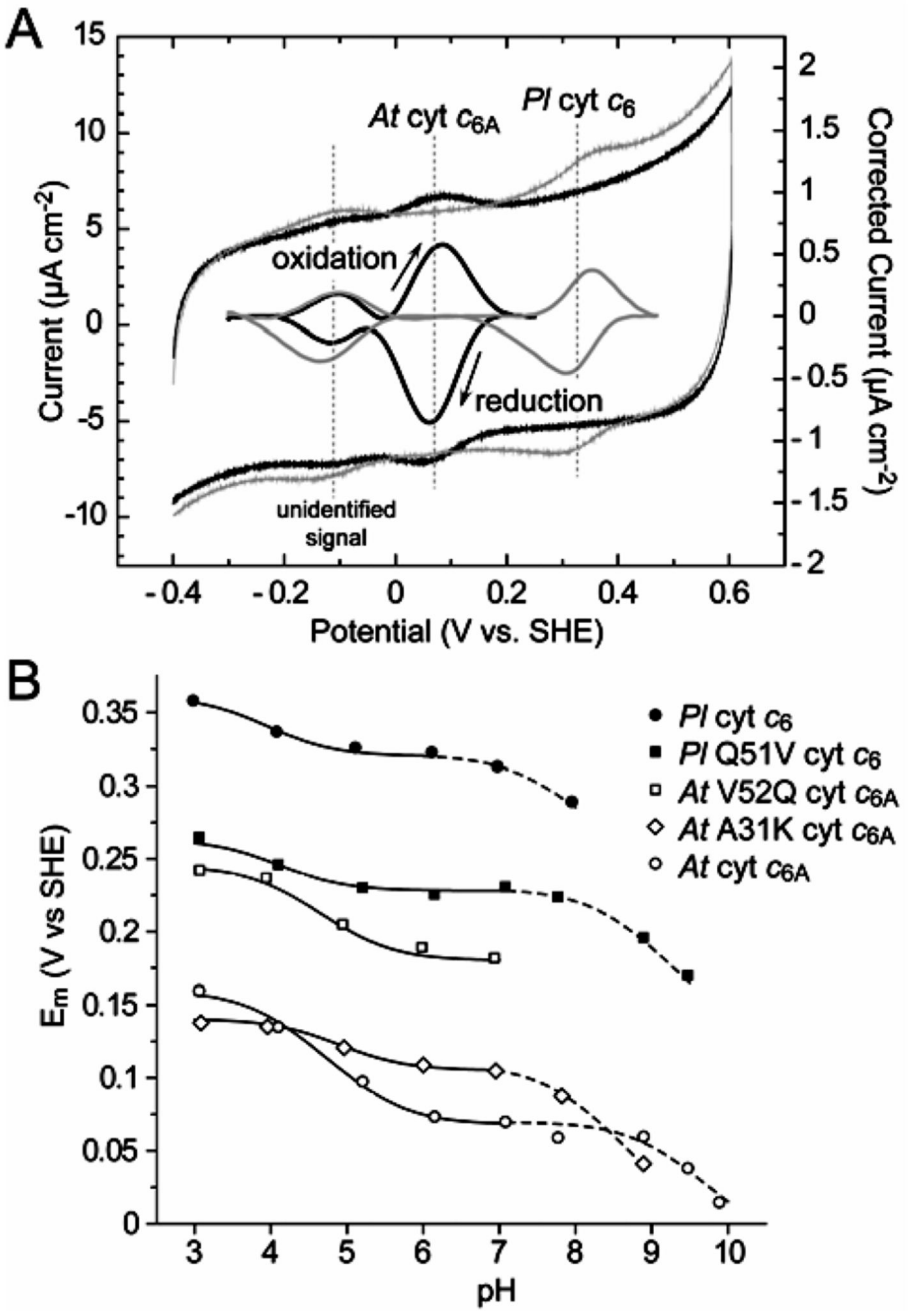

Figure 3.

(A) Cyclic voltammograms for cyt c_{6A} and cyt c_6 adsorbed on a PGE electrode, *A. thaliana* cyt c_{6A} (black) and *P. laminosum* cyt c_6 (gray), with their background corrected signals. The high potential redox couple is characteristic for protein-bound heme, whereas the low potential redox couple is from an unidentified contaminant (which is not visible on SDS gels and, hence, constitutes a small percentage of protein present but appears to react better with the electrode). Conditions: pH 7.1, scan rate 50 mV s^{-1}, 25 °C. (B) pH dependence of the midpoint potentials (E_m) at 25 °C. The data are fitted using the Nernst equation, $E_m = E$

$_{acid} - RT/F \ln[(1 + K_{ox}/a_{H+})/(1 + K\text{red}/a_{H+})]$, where E_{acid} is the pH-independent value at low pH for pK_{ox1} and pK_{red1} (solid lines) and the pH-independent value at neutral pH for pK_{ox2} (dashed lines).

Europe PMC Funders Author Manuscripts

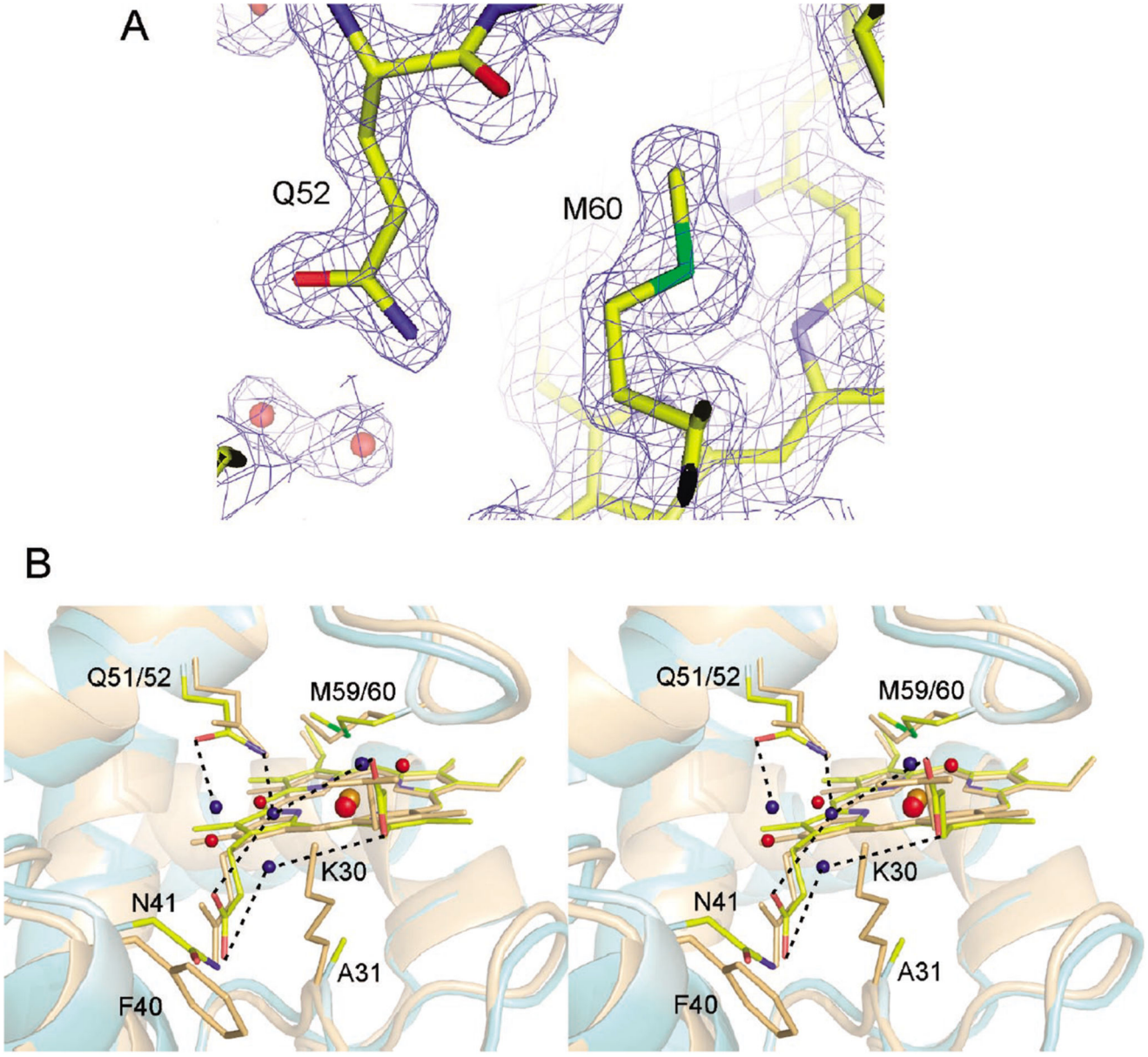

Figure 4.

(A) Part of a σ-weighted electron density map contoured at 1.0 σ for the oxidized V52Q-AA-c_{6A} variant structure of *A. thaliana.* The Gln52 and Met60 referred to in the text are indicated. (B) Stereoview of the heme regions of an overlay of reduced *P. laminosum* cyt c_6 (light orange) and the oxidized V52Q-AA-c_{6A} variant of *A. thaliana* (pale cyan). Water molecules are shown as small spheres: red for *P. laminosum* cyt *c 6* and blue for the V52Q-AA *A. thaliana* cyt c_{6A} variant. The iron atoms are shown as larger spheres: orange for *P. laminosum* and red for *A. thaliana*. Hydrogen bonding interactions are depicted by dashed lines; certain amino acids discussed in the text are labeled and shown as yellow sticks for *A. thaliana* or light orange sticks for *P. laminosum*.

Table 1

Crystallographic Data Processing and Refinement Statistics for *P. laminosum* Cytochrome c_6 and the V52Q-AA Variant of *A. thaliana* Cytochrome c_{6A}

	***Pl* cyt *c* $_6$**	**V52Q-AA *At* cyt *c* $_{6A}$**
	Data Collection and Processing	
space group	$P6_3$	$P3_221$
unit cell parameters (Å)	$a = b = 57.4$,	$a = b = 57.8$,
	$c = 89.5$	$c = 65.1$
no. of measured reflections	36 142	16 890
no. of unique reflections	11 288	16 451
-R_{merge} (%)[a]	9.6(23.1)[b]	8.6 (26.4)
average $I/\sigma(I)$	12.3 (4.8)	19.2(5.6)
multiplicity	3.2 (3.1)	7.8 (4.8)
completeness (%)	99.7(100.0)	98.9 (97.5)
	Refinement Statistics	
resolution range (Å)	25.59–2.0	50.1–1.60
	(2.05–2.00)	(1.64–1.60)
R-factor (%)	18.4(22.8)	19.8(18.1)
R_{free}-factor (%)	25.5 (30.5)	23.6 (22.6)
	Quality of Model	
rmsd bond lengths (Å)	0.019	0.013
rmsd bond angles (deg)	1.779	1.356
	Ramachandran Plot Quality	
% in most favored region	84.9	84.8
% in additional allowed region	15.1	15.2
	Model	
atoms (amino acids)	1217(chain A3–86, chain B 3–86)	929 (95)
ligands	2 hemes	heme
water molecules	116	115
B-factor (Å^2)	26.8	19.5

[a] $R_{merge} = \Sigma_i |I_i - \langle I \rangle| / \Sigma \langle I \rangle$ where $\langle I \rangle$ is the mean intensity of *N* reflections with intensities I_i and common indices *h*, *k*, and *l* (scalepack output).

[b] Values of reflections recorded in the highest resolution shell are shown in parentheses.

Europe PMC Funders Author Manuscripts

Table 2

Reduction Potentials, *pK* Values, and Spectral Data for Wild-Type and Mutant Proteins

protein	E_m(mV)[a] neutral pH	ΔE_m (vs WT)	pK_{ox1}	pK_{red1}	pK_{ox2}	α-band max (nm)
		A. thaliana cyt c_{6A}				
wild-type	+71	-	3.9	5.4	9.0	555.4
V52Q	+ 180	+ 109	4.1	5.2	n.d.	553.1
A31K	+ 105	+34	4.6	5.2	7.8	555.4
AA	+83	+12	3.7	4.9	8.8	555.4
AA-V52Q	+ 168	+97	3.6	5.1	8.5	553.1
		P. laminosum cyt c_6				
wild-type	+325	-	3.6	4.3	7.4	553.1
Q51V	+225	-100	4.0	4.6	8.3	555.5

[a] E_m, the pH-independent reduction potential at approximately neutral pH. p*K* values were determined by fitting the data in Figure 3B (see text). Errors are ±5 mV for E_m and ±0.05 for the *pK* values.

Table 3

Comparison of Heme Solvent Accessibility between *A.thaliana* Cyt c_{6A} and Cyt c_6 for Which Structures Have Been Determined with X-ray Crystallography

			solvent exposure Å^{2a}	
	Pdb code	**$E_{m,7}$(mV)**	**total heme**	**porphyrin ring^e**
	Cytochrome c_{6A}			
Arabidopsis thaliana wild-type	2dge[11]	71[b,d]/94[c,5]	70.4	15.9
I17A/G18A oxidized	2ce0[5]	83[b,d]/89[c,5]	78.9	21.6
I17A/G18A reduced	2ce1[5]		79.6	20.6
I17A/G18A/V52Q oxidized	2v07[d]	168[b,d]	97.2	19.8
	Cytochrome c_6			
Arthrospira maxima	1f1f[32]	314[c,47]	62.3	17.9
Cladophora glomerata	1ls9[48]	355 [b,48]	60.9	11.2
Chlamydomonas reinhardtii	1cyi/1cyj[31]	370[c,49]	70.0	9.4
Monoraphidium braunii	1ctj[16]	358[c,50]	60.7	7.4
Phormidium laminosum	2v08[d]	325[b,d]	57.7	14.7
Porphyra yezoensis	1gdv[51]		52.1	10.1
Scenedesmus obliquus				
oxidized	1c6o[4]		73.6	8.8
reduced	1c6r[4]		67.4	12.0

[a] Calculated with NACCESS.[52] [b] Obtained by CV. [c] Potentiometric titration. [d] Present work. [e] Cβ, O_1, and O_2 atoms were excluded from the calculation.